Electronic Supplementary Material (ESI) for Sustainable Energy & Fuels.

Supplementary Information

Sustainable production of ethylene from bioethanol over hierarchical ZSM-5 nanosheets

Sirawit Shetsiri[a‡], Anawat Thivasasith[a‡], Wannaruedee Wannapakdee[a], Kachaporn Saenluang[a], Piraya Wetchasat[a], Saros Salakhum[a], Somkiat Nokbin[b], Jumras Limtrakul[c] and Chularat Wattanakit[*,a]

[a]Department of Chemical and Biomolecular Engineering, School of Energy Science and Engineering and Nanocatalysts and Nanomaterials for Sustainable Energy and Environment Research Network of NANOTEC, Vidyasirimedhi Institute of Science and Technology, Rayong 21210, Thailand

[b]Department of Chemistry, Faculty of Science, Kasetsart University, Bangkok 10900, Thailand

[c]Department of Materials Science and Engineering, School of Molecular Science and Engineering, Vidyasirimedhi Institute of Science and Technology, Rayong 21210, Thailand

*E-mail: chularat.w@vistec.ac.th

Author Contributions: ‡These authors contributed equally.

Table S1 Summarized information of the catalytic performances for the ethanol dehydration to ethylene.

Catalysts	Ethanol conversion (%)	Ethylene selectivity (%)	Reaction temperature (°C)	LHSV[a]/ WHSV[b]/ GHSV[c] (h^{-1})	Lifespan, Stability (h)	Ref.
Oxide catalyst						
γ-Al_2O_3	90.1	78.7	450	3[a]	~80	1
TiO2/γ-Al_2O_3	100	99.4	360-500	26-234[a]	~400	2
Molecular sieve-catalyst						
ZSM5-DeAl-1/25	98.1	100	220	2.5[b]	>100	3
ZSM5-DeAl-1/25	96.3	100	220	1.5[c]	>100	3
ZSM5-DeAl-1/50	98.3	100	240	1.5[c]	60	3
ZSM5-DeAl-1/100	98.9	99.9	240	1.5[c]	50	3
HZSM-5	99	99	260	1.1[a]	~400	4
3%La-HZSM-5	98.5	99.5	260	1.1[a]	>830	4
HZSM-5	97.3	93.7	300	3[a]	~60	1
0.5%La-2%P-HZSM-5	100	99.9	240-280	2[b]	>70	5
SAPO-34	93.5	86.0	350	3[a]	~100	1
NiAPSO-34	96.5	92.3	350	3[a]	~100	1
Nano-CAT	100	99.7	240	1[b]	~630	6
TPA-MCM-41	98	99.9	300	2.9[b]	n/a	7
STA-MCM-41	99	99.9	250	2.9[b]	n/a	8
TRC-92	70	99.0	280	2.9[b]	n/a	9
Heteropolyacid catalyst						
$Ag_3PW_{12}O_{40}$	100	99.2	220	6000[c]	n/a	10
Commercial catalyst						
SynDol(Halcon) (SD,USA)	99	96.8	450	26-234[a]	-	2,11

[a]LHSV: liquid hourly space velocity, [b]WHSV: weight hourly space velocity, [c]GHSV: gas hourly space velocity

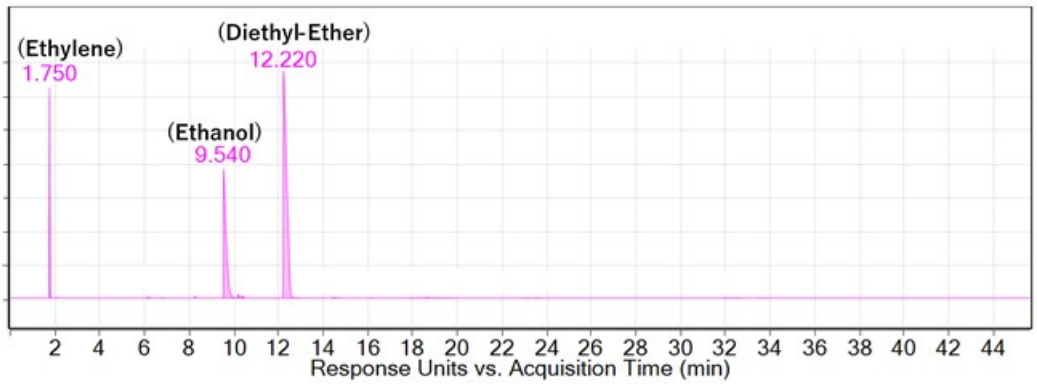

Fig. S1 GC chromatogram with FID signal (a. u) as a function of retention time (RT) of the reaction mixture.

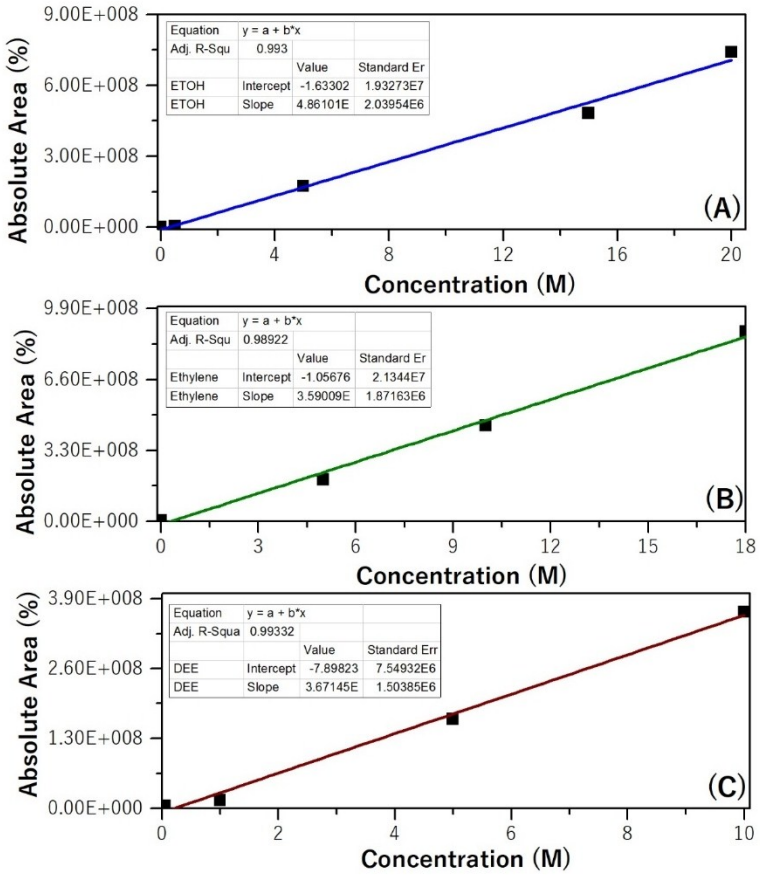

Fig. S2 Calibration curves of (A) ethanol, (B) ethylene, and (C) diethylether plotted by using the absolute area as a function of the concentration of each compound.

Table S2 Calculated data of all synthesized samples obtained from XRD, SEM and TEM techniques

Samples	**Relative crystallinity (%)[a]**	**Average crystallite size (nm)**	**Average particle size (nm)**	**Average sheet thickness (nm)**
MFI-CON(38)	100.00	118.48	362.50	-
MFI-HieNS(37)	91.09	29.87	224.09	8.14
MFI-HieNS(75)	92.22	30.08	240.10	8.72
MFI-HieNS(103)	93.35	33.04	252.69	8.63
MFI-HieNS(159)	96.51	33.99	255.87	9.06

[a] Relative crystallinity (%) = "crystallinity of zeolite sample (%)／crystallinity of reference (MFI-CON(38)) (%)".

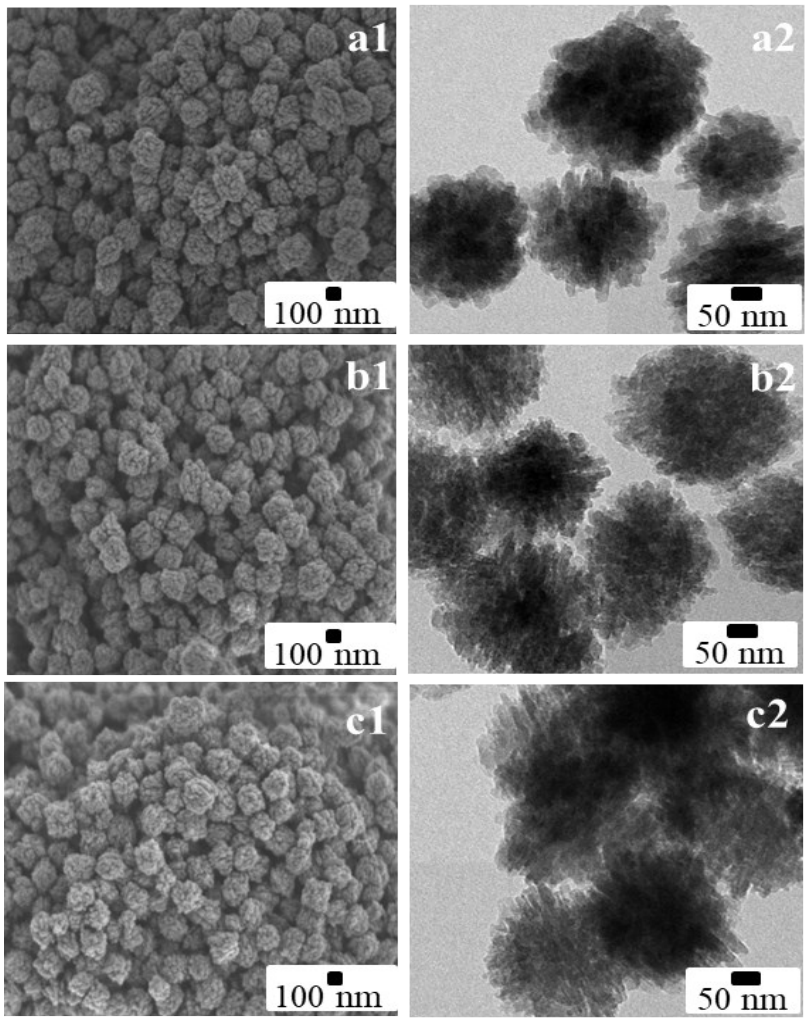

Fig. S3 SEM and TEM images of (a1-a2) MFI-HieNS(75), (b1-b2) MFI-HieNS(103), and (c1-c2) MFI-HieNS(159).

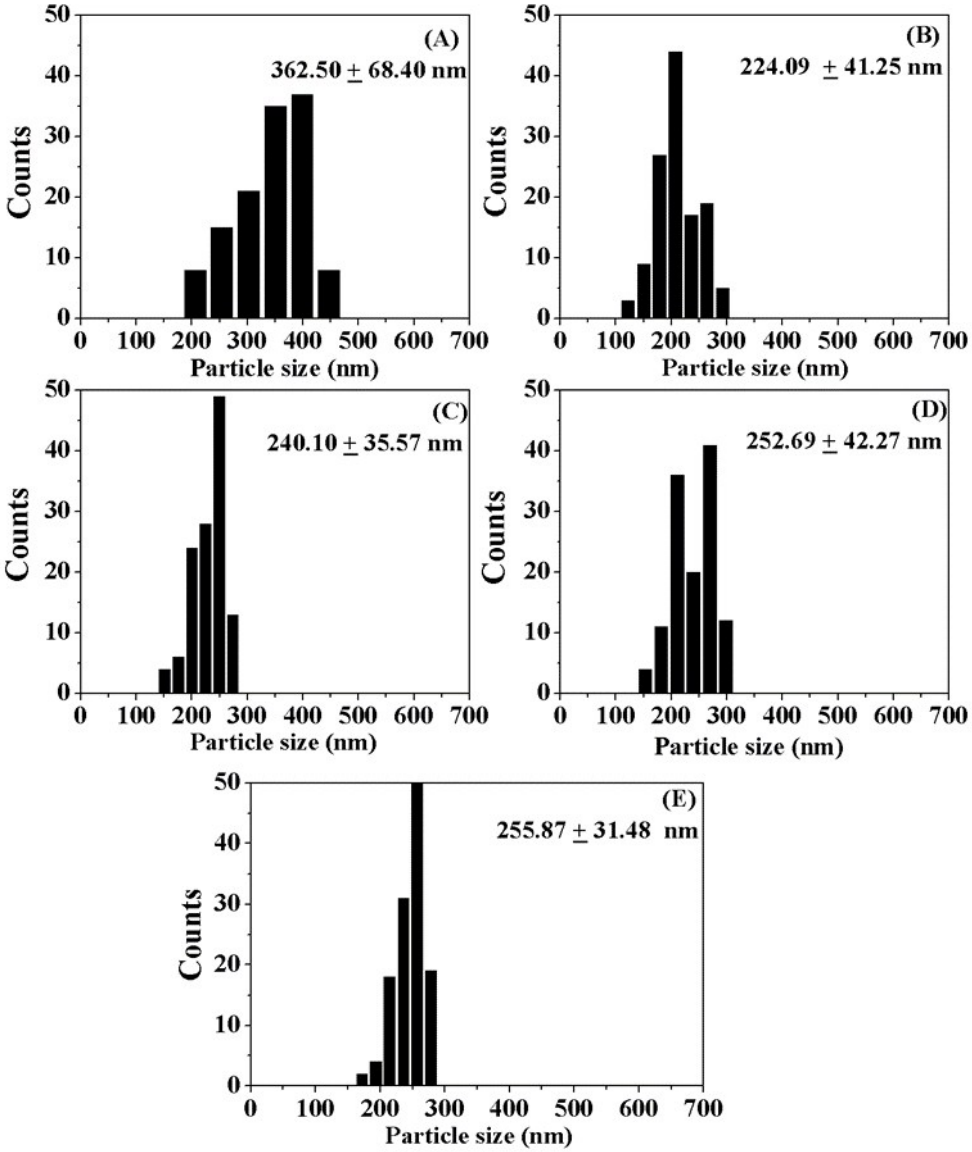

Fig. S4 Particle size distribution of (A) MFI-CON(38), (B) MFI-HieNS(37), (C) MFI-HieNS(75), (D) MFI-HieNS(103), and (E) MFI-HieNS(159).

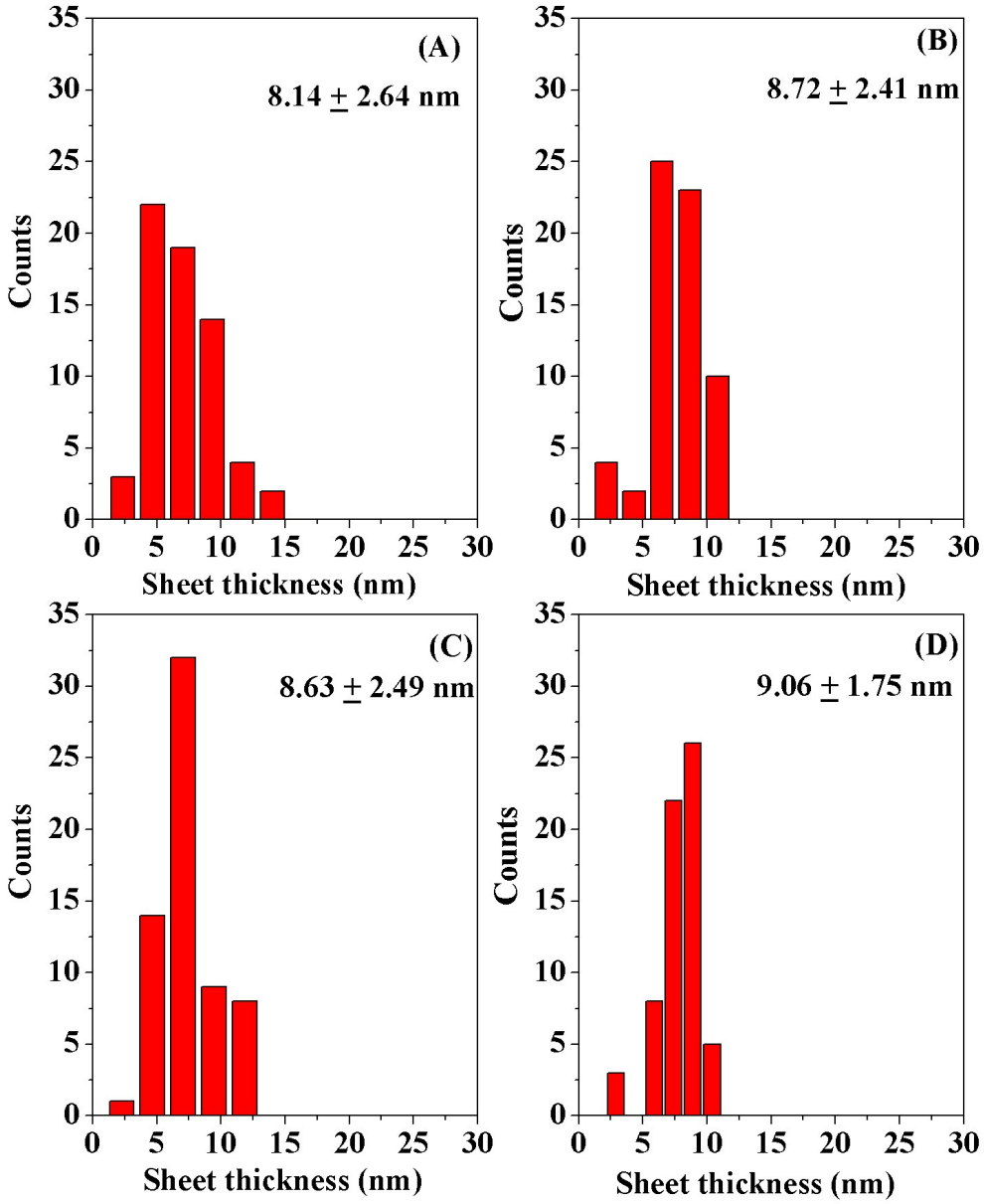

Fig. S5 Thickness of nanolayers distribution of (A) MFI-HieNS(37), (B) MFI-HieNS(75), (C) MFI-HieNS(103), and (D) MFI-HieNS(159).

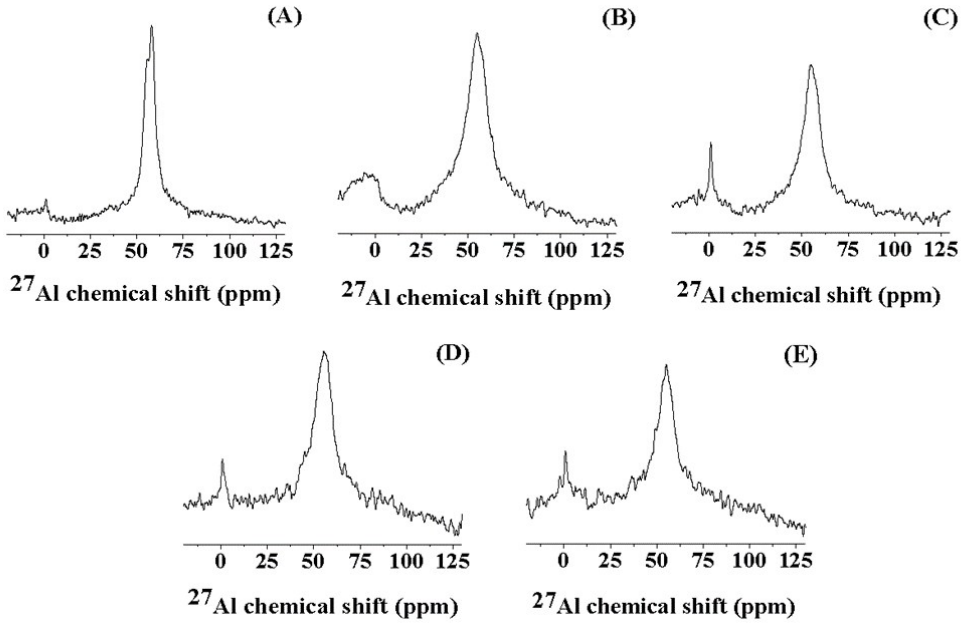

Fig. S6 ^{27}Al-NMR spectra of (A) MFI-CON(38), (B) MFI-HieNS(37), (C) MFI-HieNS(75), (D) MFI-HieNS(103), and (E) MFI-HieNS(159).

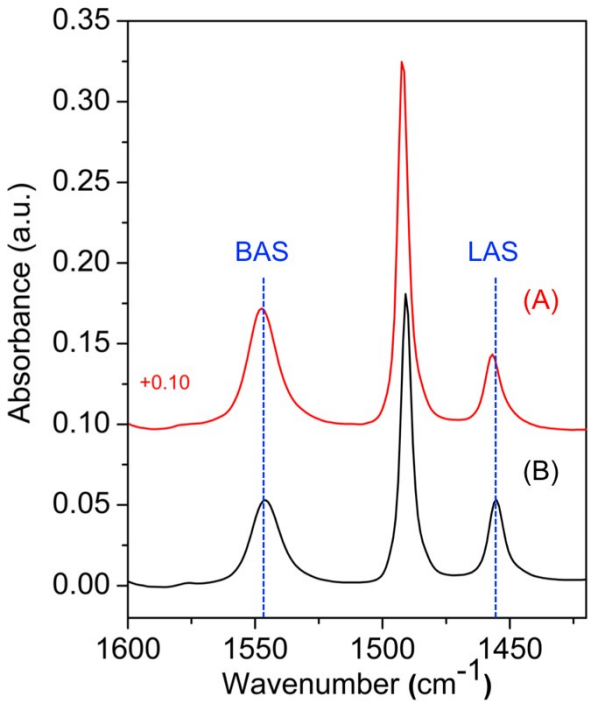

Fig. S7 Pyridine-IR spectra of (A) MFI-CON(75) and (B) MFI-HieNS(75) obtained at 423 K.

Table S3 Concentration of acid sites in conventional HZSM-5 (MFI-CON (75)) and HZSM-5 nanosheets (MFI-HieNS (75))

Catalysts	[BAS] µmol/g	[LAS] µmol/g
MFI-CON (75)	171	51
MFI-HieNS (75)	150	62

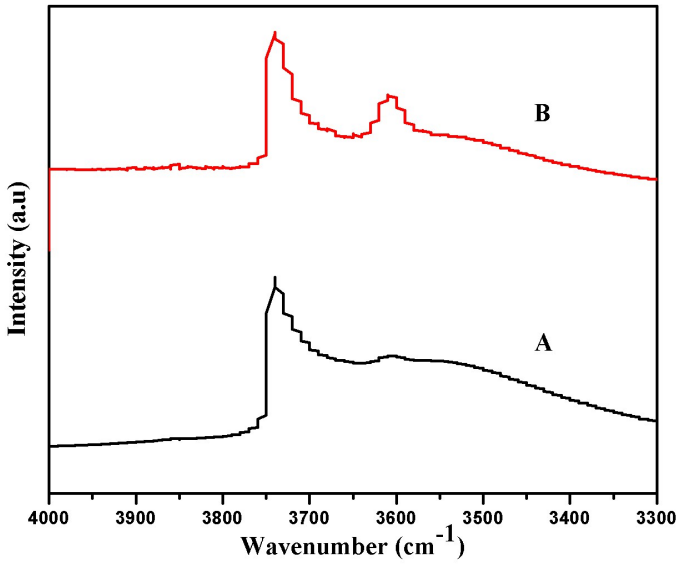

Fig. S8 FTIR spectra in the O-H stretching region of: (A) the hierarchical ZSM-5 and (B) the conventional ZSM-5.

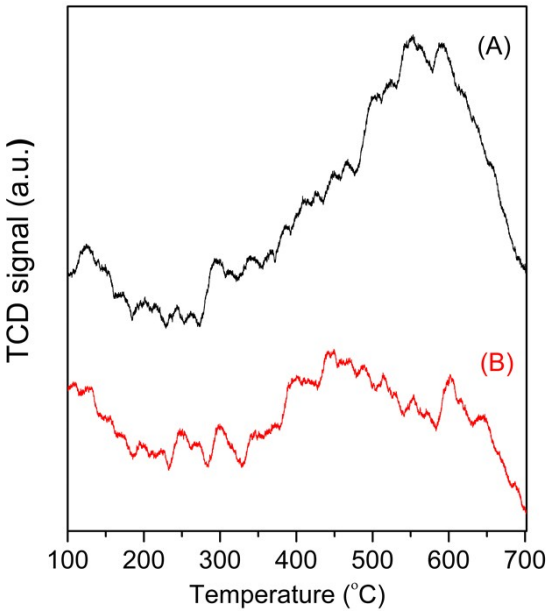

Fig. S9 O_2-TPO profiles of (A) MFI-CON(38) and (B) MFI-HieNS(37).

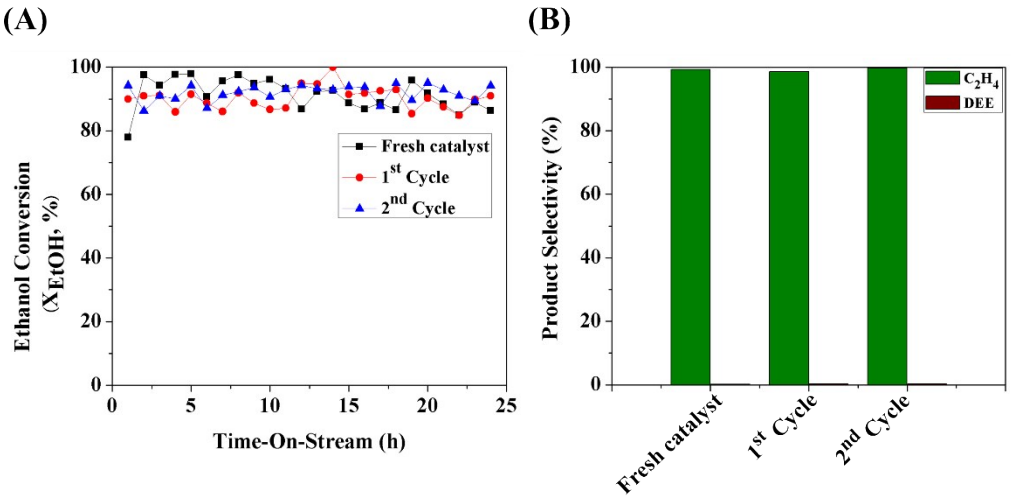

Fig. S10 (A) Ethanol conversion as a function of time-on-stream (TOS) and (B) selectivity of products obtained at 15 h of TOS with the catalysts generated by one and two cycles at 350˚C, WHSV of 10 h^{-1}, and the molar ratio of N_2 to EtOH of 2.5:1 over the MFI-HieNS(75) catalyst.

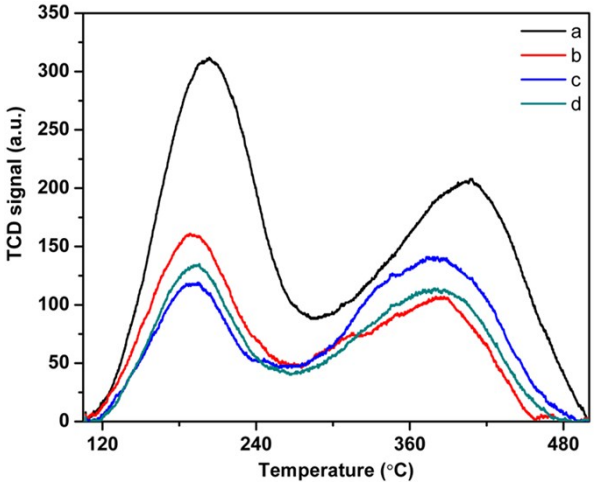

Fig. S11 NH_3-TPD profiles of a) fresh MFI-CON(38), b) MFI-CON(38) obtained after 2nd cycle of the regeneration, c) fresh MFI-HieNS(75) and d) MFI-HieNS(75) after 2nd cycle of the regeneration.

Table S4 Acidic properties obtained by NH_3-TPD technique of fresh and spent catalysts.

Sample	Desorption Temperature (°C)		Acidity amount (μmol.g^{-1})		
	LOW DES	High DES	Weak	Strong	Total
Fresh-MFI-CON(38)	203	407	146	154	300
MFI-CON(38)	188	387	62	74	136
after 2nd cycle of regeneration					
Fresh- MFI-HieNS(75)	194	392	47	149	196
MFI-HieNS(75)	196	393	35	54	89
after 2nd cycle of regeneration					

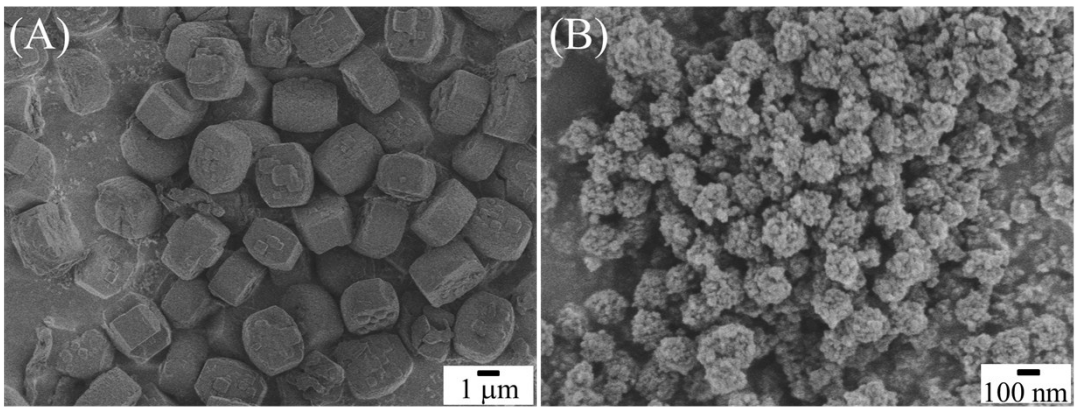

Fig. S12 SEM images of a) spent MFI-CON(38) and b) spent MFI-HieNS(75) after 2nd cycle of regeneration

Table S5 The composition of organic compounds in the starting bioethanol solution identified by GC-MS technique equipped with a capillary column (HP-5MS 5% Phenyl Methyl Silox, 30 m x 250 µm x 0.25 mm), and GC-MS condition of temperature profiles in the range of 40 to 200 °C and holding time of 40 min.

No.	RT(min)	Identity Compounds	Structure	%Mass
1	1.677	Ethanol	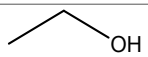	98.33
2	1.792	Isopropyl alcohol	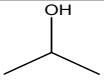	0.45
3	2.012	1-Propanol	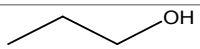	0.03
4	2.274	Nitrous Oxide	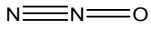	0.01
5	2.383	Ethyl Acetate	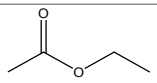	0.02
6	2.477	2-Methyl-1-Propanol	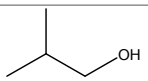	0.57
7	2.747	2-Methoxy-Ethanamine	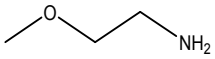	0.15
8	4.069	1,1-diethoxy-Ethane	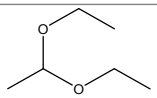	0.16
9	4.229	N-Methylene-Ethanamine	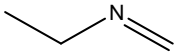	0.03
10	4.991	Toluene	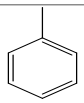	0.25

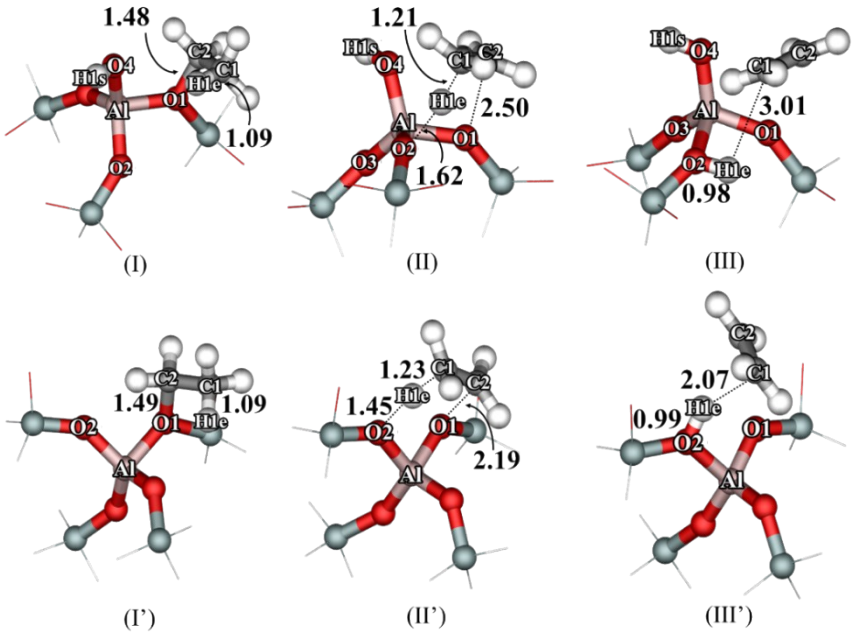

Fig. S13 Optimized structures of ethoxide intermediates and transition states as well as the ethoxide conversion to ethylene over the Brønsted acid site at external surfaces (I-III) and the Brønsted acid site located at the internal surface (I'-III') of MFI zeolite.

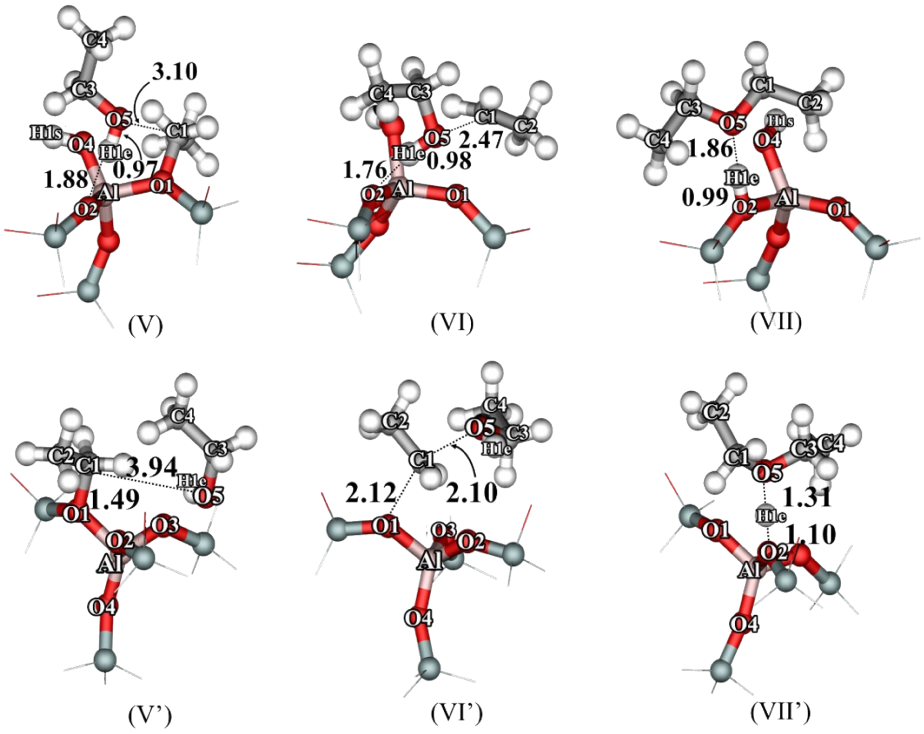

Fig. S14 Optimized structures of ethoxide intermediates and transition states as well as the ethoxide conversion to DEE over the Brønsted acid site at external surfaces (V-VII) and the Brønsted acid site located at internal surface (V'-VII') of MFI zeolite.

References

[1] X. Zhang, R. Wang, X. Yang and F. Zhang, *Micropor. Mesopor. Mater.*, 2008, **116**, 210-215.

[2] G. Chen, S. Li, F. Jiao and Q. Yuan, *Catal. Today*, 2007, **125**, 111-119.

[3] C.-Y. Wu and H.-S. Wu, *ACS Omega*, 2017, **2**, 4287-4296.

[4] J. Ouyang, F. Kong, G. Su, Y. Hu and Q. Song, *Catal. Lett.*, 2009, **132**, 64-74.

[5] N. Zhan, Y. Hu, H. Li, D. Yu, Y. Han and H. Huang, *Catal. Commun*., 2010, **11**, 633-637.

[6] J. Bi, X. Guo, M. Liu and X. Wang, *Catal. Today*, 2010, **149**, 143-147.

[7] A. Ciftci, D. Varisli, K. Cem Tokay, N. Aslı Sezgi and T. Dogu, *Chem. Eng. J.*, 2012, **207-208**, 85-93.

[8] D. Varisli, T. Dogu and G. Dogu, *Ind. Eng. Chem. Res.*, 2008, **47**, 4071-4076.

[9] D. Varisli, T. Dogu and G. Dogu, *Chem. Eng. Sci.*, 2010, **65**, 153-159.

[10] J. Gurgul, M. Zimowska, D. Mucha, R. P. Socha and L. Matachowski, *J. Mol. Catal. A Chem*., 2011, **351**, 1-10.

[11] N. K. Kochar, R. Merims and A. S. Padia, 1981, **77**, p 66-70.